



StegResNet: A Residual Learning-Based Lightweight Framework for Robust Spatial Image Steganalysis

Neelam Swarnkar^{*1}, Ani Thomas²

^{*1}Department of Computer Science and Engineering, Chhattisgarh Swami Vivekananda Technical University, Durg, 490021, India email: neelamswarnkarnit@gmail.com, Orcid Id: 0000-0002-9940-4034,

²Department of Information Technology, Bhilai Institute of Technology, Durg, 490021, India

Citation: Neelam Swarnkar, et.al (2024). StegResNet: A Residual Learning-Based Lightweight Framework for Robust Spatial Image Steganalysis, *Educational Administration: Theory and Practice*, 30(6) 5486-5499

Doi: 10.53555/kuey.v30i6.11054

ARTICLE INFO

Received: 6 June 2024

Accepted: 11 June 2024

ABSTRACT

Steganalysis, the process of detecting hidden information within digital images, presents persistent challenges due to the imperceptible and adaptive nature of modern steganographic algorithms. To address these challenges, this study introduces StegResNet, a customized deep residual learning model specifically designed for spatial domain image steganalysis. Built upon the pretrained ResNet18 architecture, StegResNet employs transfer learning to leverage generalized visual representations from ImageNet while fine-tuning deeper layers to learn embedding-specific residual features. The architecture incorporates residual connections, batch normalization, and a lightweight binary classification head, enabling effective preservation of low-level noise features essential for detecting subtle embedding distortions. Experimental evaluation was conducted using a composite dataset formed by merging BOSSBase v1.01 and BOWS2, with stego images generated through five spatial content adaptive steganographic algorithms HUGO, HILL, WOW, S-UNIWARD, and MiPOD at payloads of 0.2 bpp and 0.4 bpp. The proposed model achieved an overall detection accuracy of 91.27%, outperforming several state-of-the-art CNN-based steganalyzers such as YeNet, YedroudNet, ZhuNet, SRNet and GBRASNet. Analysis of the confusion matrix and performance metrics confirmed high precision, recall, and F1-scores, demonstrating strong generalization and robustness. The results substantiate that the proposed StegResNet framework effectively bridges residual learning and steganalysis, offering an efficient, interpretable, and high-performing solution for detecting hidden payloads in grayscale images.

Keywords: Image steganalysis, Deep residual learning, Transfer learning, ResNet18, Spatial domain steganalysis

1. Introduction

In the digital era, where vast volumes of data are transmitted across diverse communication platforms, ensuring information security has become a critical concern. Among the methods developed to safeguard sensitive information, steganography and steganalysis have gained significant attention. Steganography is the art of concealing data within digital media such as images, audio, or video to mask its existence from unintended observers. This covert communication technique relies on embedding information in a way that preserves perceptual invisibility. Conversely, *steganalysis* aims to detect and analyse hidden data within such media, ensuring the integrity and authenticity of digital communication. As steganographic algorithms evolve to produce increasingly imperceptible embedding artefacts, there arises a parallel demand for more sophisticated and robust steganalysis techniques.

Traditional image steganalysis approaches primarily relied on handcrafted features and heuristic statistical methods. While such techniques provided reasonable detection performance against simple embedding schemes, they often failed to generalize across different steganographic algorithms and payloads. The advent of deep learning has revolutionized this field, introducing powerful data-driven models capable of learning complex spatial correlations and noise patterns inherent to stego content. Convolutional Neural Networks (CNNs), in particular, have demonstrated remarkable success in automating feature extraction and improving

detection accuracy. A variety of CNN-based architectures such as YeNet [8], YedroudjNet [9], SRNet [10], ZhuNet [11], and GBRASNet [12] have been proposed to enhance detection precision and robustness across multiple embedding algorithms and payload conditions.

Despite these advancements, there has been a lack of research into lightweight CNN architectures that balance accuracy and computational efficiency for image steganalysis tasks. Research in spatial-domain image steganalysis increasingly integrates attention mechanisms and transformer-based designs to enhance feature discrimination within lightweight networks. While conventional CNNs capture local residual cues, they often miss global dependencies essential for detecting subtle embedding artefacts. Hybrid frameworks, such as the convolutional vision transformer [40], combine self-attention with convolutional backbones to jointly exploit local and global context. Concurrently, depthwise separable convolutions, channel/spatial attention, and SE-based pruning are employed to minimize parameters and inference cost, achieving a balance between accuracy, efficiency, and contextual sensitivity in steganalysis. Compared to deep learning's baseline models, shallow CNN models have demonstrated effectiveness in improving results across various applications, including image classification tasks.

The primary goal of the experiments conducted is to utilize lightweight CNNs based on validated pre-trained deep learning models to accurately classify stego and cover images while minimizing computational overhead and ensuring strong generalization across various datasets and spatial domain steganography algorithms. To the best of the authors' knowledge, no prior studies have implemented residual learning [2] and transfer learning [4-6,37] from the ResNet18 deep model for universal spatial image steganalysis. The authors have developed a lightweight residual learning based architecture called StegResNet, for content-adaptive [7] spatial domain image steganalysis. The proposed model adapts the ResNet18 backbone pretrained on the ImageNet dataset to detect subtle embedding distortions in grayscale images. By leveraging transfer learning, StegResNet effectively transfers generalized visual features from natural images to the steganalysis domain. The main motivation of this proposed work is to design a CNN based universal steganalyzer capable of identifying stego images generated by a variety of content-adaptive steganographic techniques with varying payloads. The proposed CNN based steganalyzer is introduced and detailed in Section 3.

The key contributions of the proposed novel work are outlined below:

1. We introduce a novel StegResNet architecture by tailoring the residual learning mechanism of ResNet18 for Spatial domain steganalysis, enabling the preservation of fine-grained embedding distortions that are typically lost in conventional CNNs.
2. We employ pretrained ImageNet weights for efficient feature transfer, freezing early layers to retain generic image features and fine tuning deeper layers to extract subtle steganographic patterns.
3. We develop a diverse dataset to improve generalization, incorporating a variety of steganographic techniques and payload sizes to ensure the model can detect a wide range of embedding methods.
4. We conducted extensive experimental validation, including confusion matrix evaluation, convergence analysis, and comparative benchmarking, which confirmed the model's strong generalization, low detection error rate, high accuracy, and suitability for practical steganalysis applications.

The remaining sections of the paper are structured as follows: Section 2 reviews the foundational works in the development of CNN-based steganalyzers. Section 3 details the proposed framework. Section 4 presents and analyses the experimental results. Finally, Section 5 concludes the paper and discusses potential directions for future research.

2. Literature review

Image steganalysis plays an essential role in digital forensics and information assurance, aiming to detect concealed information hidden within digital images. Traditional steganalysis methods primarily relied on handcrafted statistical feature extraction, leveraging statistical and perceptual attributes such as Image Quality Measures (IQMs) [14] and image moments [15] and classical machine learning classifiers. While these handcrafted approaches demonstrated competitive performance against specific steganographic algorithms, they were inherently limited in generalization across varying embedding schemes, image sources, and payload capacities. These steganalysis methods were classified into specific and universal steganalysis. Specific steganalysis algorithms targeted individual embedding schemes [5], while universal algorithms generalized across multiple embedding strategies using statistical descriptors and supervised learning [6]. Traditional features such as the binary similarity measure [7], Discrete Cosine Transform (DCT) [8,9], wavelet coefficients [10], and co-occurrence matrices [11] formed the basis of these detectors. Later, higher-order statistics, such as SPAM [12] and Rich Models (SRM) [13–15], improved accuracy by modeling inter-pixel correlations. However, these rich-model-based methods often suffered from excessive dimensionality (tens of thousands of features), long training times, and susceptibility to overfitting. Moreover, feature construction demanded domain expertise, limiting scalability and automation.

The emergence of deep learning particularly Convolutional Neural Networks (CNNs), revolutionized steganalysis by enabling end-to-end learning of hierarchical spatial dependencies without manual feature design [16–19]. CNN-based approaches significantly improved detection accuracy by hierarchically capturing complex residual dependencies and subtle embedding artefacts within spatial or transform domains. Subsequent architectural enhancements introduced innovations such as diverse activation functions [17–18], depthwise separable convolutions [19], spatial pyramid pooling [20], selection-channel awareness [21], skip connections [22], hybrid and attention-based network designs [23–25], and advanced data augmentation techniques [26–28]. Despite these improvements, the high computational demands and increasing architectural depth of CNN models continue to challenge efficiency and real-time applicability, particularly for high-resolution image datasets.

This section presents a detailed review of five SOTA CNN-based steganalyzers QianNet, XuNet, YeNet, YedroudjNet, SRNet, ZhuNet, and GBRASNet that have significantly influenced modern Spatial domain image steganalysis. Qian et al.[3] introduced the first CNN-based steganalyzer QianNet or GNCNN using Gaussian activation and high-pass filtering, achieving performance close to SRM [21] and higher than SPAM[12]. Xu et al. [22] introduced XuNet enhanced statistical modeling with an absolute-value (ABS) layer and 1×1 convolutions, improving detection of S-UNIWARD and HILL. Ye et al. [8] developed YeNet wherein it initialized its convolutional filters using SRM high-pass kernels and introduced the Truncated Linear Unit (TLU) activation to suppress image content while preserving embedding signals. Yedroudj et al.[9] introduced YedroudjNet integrated SRM-inspired pre-processing, batch normalization, and an expanded fully connected section, resulting in notable accuracy gains. ZhuNet et al. [11] incorporated separable convolutions and Spatial Pyramid Pooling (SPP) to support arbitrary image sizes, achieving significant improvement over its predecessors. Boromound et al. [10] developed SRNet, advanced further with a deep residual design eliminating pooling in the front-end, achieving state-of-the-art results for both spatial and JPEG domains. The latest advancement, GBRASNet [12], builds upon prior architectural foundations while introducing novel elements such as the $3 \times \text{TanH}$ activation function and the use of depthwise-separable convolutions. By focusing on lightweight feature extraction and efficient global average pooling, GBRASNet attains high detection accuracy with significantly reduced computational overhead, establishing itself as one of the most computationally efficient steganalyzers in the spatial domain to date.

Table 1 presents a comparative analysis of key CNN-based spatial-domain steganalysis models, highlighting their architectural characteristics, datasets, tested algorithms, feature extraction strategies, and corresponding detection performances.

Table 1. Comparative summary of SOTA CNN-based steganalysis architectures

Model	Key Architectural Features	Activation Function	Preprocessing ,Dataset(s)	Algorithms Tested	Detection Error Rate	Reported Detection Performance / Remarks
QianNet (2015) [3]	5-layer CNN with Gaussian activation and average pooling	Gaussian	BOSSBase (256×256)	HUGO, WOW, S-UNIWARD	10% higher than SPAM ; GNCNN: HUGO (28.9%), WOW (29.3%), S-UNIWARD (30.9%) SPAM: HUGO (39.1%), WOW (38.2%), S-UNIWARD (35.1%)	Foundational CNN model
XuNet (2016) [22]	5-layer CNN with ABS layer and 1×1 convolutions; enhanced statistical modeling	TanH	Noise-residual input, BOSSBase (512×512)	S-UNIWARD, HILL	Accuracy : 0.1 bpp: CNN: HILL (58.44%) S-UNIWARD (57.33%) SRM: HILL (56.44%) S-UNIWARD (59.25%) 0.4 bpp: CNN: HILL (79.24%) S-UNIWARD (80.24%) SRM: HILL (75.47%) S-UNIWARD (79.53%)	Comparable to SRM+EC; better generalization
YeNet (2017) [8]	SRM-initialized filters, 8-layer CNN, selection-channel awareness	TLU	SRM high-pass filter set, BOSSBase (256×256)	WOW, HILL, S-UNIWARD	0.4 bpp CNN: WOW (9.59%) S-UNIWARD (12.81%) HILL (17.08%) SRM: WOW (15.36%) , S-UNIWARD (21.36%), HILL(24.10)	Outperforms maxSRMd2 and SRM; robust spatial detection

Yedroud jNet (2018) [9]	SRM filter-bank preprocessing, BN + scale layer, expanded FC section	TLU	SRM filter bank, BOSSBase, BOWS2	WOW, S-UNIWARD	0.2 bpp: CNN: WOW (27.8%) S-UNIWARD (36.7%) SRM: WOW (36.5%) S-UNIWARD (36.6%) 0.4 bpp: CNN: WOW (14.1%) S-UNIWARD (22.8%) SRM: WOW (25.5%) S-UNIWARD (24.7%)	Superior to SRM+EC and YeNet; reduced error probability
ZhuNet (2019) [11]	3×3 kernels, depthwise separable convs, Spatial Pyramid Pooling (SPP)	ReLU	SRM-inspired preprocessing, BOSSBase, BOWS2	WOW, S-UNIWARD	On BOSSBase v1.01: 0.2 bpp: CNN: WOW (23.3%) S-UNIWARD (28.5%) SRM: WOW (36.5%) S-UNIWARD (36.6%) 0.4 bpp: CNN: WOW (11.8%) S-UNIWARD (15.3%) SRM: WOW (25.5%) S-UNIWARD (24.7%) CNN on BOSSBase +BOWS2 (train) BOSSBase (test): WOW(13.1% at 0.2bpp; 6.5% at 0.4bpp) S-UNIWARD(17.1% at 0.2 bpp ; 8.1% at 0.4 bpp)	Outperforms XuNet, YeNet, and YedroudjNet; SPP enhances scalability
SRNet (2019) [10]	Deep residual architecture, no pooling in early layers, universal detection	ReLU	Noise residual computation	Spatial + JPEG stego	Accuracy: On 0.2 bpp: HUGO (67.1%) HILL (65.2%), MiPOD (64.3%) On 0.4 bpp: HUGO (78.7%) HILL (75.8%), MiPOD (75.1%)	State-of-the-art accuracy; domain-agnostic performance
GBRASNet (2021) [12]	Global residual attention sub-network; multi-scale fusion	ReLU	Attention-based feature extraction, BOSSBase, BOWS2	WOW, HILL, S-UNIWARD	Accuracy: On 0.2 bpp: HUGO (74.6%) WOW (80.3%), S-UNIWARD (73.6%), HILL (68.5%), MiPOD (68.3%) On 0.4 bpp: HUGO (84.5%) WOW (89.8%), S-UNIWARD (87.1%), HILL (81.9%), MiPOD (81.4%)	efficient attention mechanism

The reviewed CNN-based steganalysis approaches demonstrate that model efficacy is highly dependent on architectural design, pre-processing strategies, and feature normalization mechanisms. Although deep models such as SRNet and GBRASNet deliver strong detection accuracy, their high computational demands limit scalability and real-time deployment. Furthermore, the minimal use of transfer learning in existing frameworks constrains generalization and slows convergence, as most models are trained from scratch. While increased depth enhances feature representation, it also amplifies overfitting risks and reduces interpretability, particularly with limited steganalysis datasets.

These limitations highlight a clear research gap the need for lightweight, residual learning–based architectures capable of efficiently extracting discriminative spatial features while maintaining sensitivity to subtle embedding artifacts. To bridge this gap, the present study introduces StegResNet, a residual learning–driven framework optimized for spatial-domain image steganalysis. By extending the ResNet18 backbone and incorporating transfer learning from ImageNet, StegResNet preserves high-frequency stego cues, stabilizes gradient flow, and accelerates convergence. Through fine-tuning its upper layers for binary classification, the

model achieves a 91.27% detection accuracy on the combined BOSSBase and BOWS2 datasets, surpassing existing CNN-based steganalyzers in accuracy, efficiency, and generalization across diverse embedding algorithms and payloads.

3. Proposed methodology

The proposed StegResNet framework, illustrated in Figure 1, is a universal deep learning architecture for spatial-domain image steganalysis, developed on the ImageNet-pretrained ResNet18 backbone and implemented in PyTorch. It effectively integrates residual learning and transfer learning principles to detect imperceptible embedding artefacts in grayscale images. The input images from the BOSSBase1.01 and BOWS2 datasets are resized from 512×512 to 224×224 pixels for compatibility with the pretrained network. To adapt ResNet18 for binary steganalysis, the original fully connected layer is replaced by a dropout–softmax classification head, enabling robust two-class decision-making. In this configuration, the early convolutional layers remain frozen to retain generic spatial representations such as edges and textures, while the deeper layers are fine-tuned to capture embedding-specific distortions and residual noise patterns. The network employs CrossEntropyLoss as the objective function and is optimized using stochastic gradient descent (SGD) with a momentum of 0.9, a learning rate of 0.001, a batch size of 32, and training over 15 epochs, amounting to approximately 11.18 million parameters.

Architecturally, StegResNet incorporates residual blocks consisting of convolutional layers, batch normalization, and skip connections, expressed mathematically by eq. (1),

$$y = F(x, \{W_i\}) + x \quad (1)$$

where $F(x, \{W_i\})$ denotes the nonlinear transformations applied by the convolutional layers. These skip connections allow the direct propagation of input (x) to deeper layers, preserving low-level spatial information while mitigating vanishing gradients. This residual mechanism ensures the retention of subtle noise patterns crucial for steganographic detection. The feature refinement mechanism leverages transfer learning by utilizing the pretrained convolutional filters of ResNet18; frozen shallow layers capture universal image statistics, whereas fine-tuned deeper layers specialize in detecting embedding artefacts such as pixel correlation inconsistencies and structural irregularities. The classifier is optimized for binary prediction, employing a dropout layer for regularization and a softmax neuron for class probability estimation, ensuring improved inter-class discrimination.

In terms of computational efficiency, StegResNet achieves an optimal trade-off between depth and complexity, with batch normalization stabilizing feature distribution and accelerating convergence. Its lightweight configuration yields rapid training and inference while maintaining high representational power making it suitable for large-scale or near-real-time steganalysis applications. Moreover, the preservation of spatial hierarchies through localized receptive fields and residual feature reintroduction ensures that both global and local spatial cues contributing to embedding detection are retained across network layers.

By harmonizing residual learning, spatial feature preservation, and transfer-based fine-tuning, StegResNet establishes a robust and efficient paradigm for spatial steganalysis. Unlike traditional CNN-based steganalyzers that struggle to retain high-frequency noise components essential for detecting embedded payloads, this model maintains strong gradient flow and low-level detail continuity, enhancing sensitivity to subtle embedding traces. Empirical evaluations on the combined BOSSBase v1.01 and BOWS2 datasets demonstrate that StegResNet attains a detection accuracy of 91.27%, outperforming leading state-of-the-art architectures such as QianNet, XuNet, YeNet, YedroudjNet, SRNet, ZhuNet, and GBRASNet. With its compact design, strong discriminative capability, and superior generalization across multiple steganographic algorithms and payloads, StegResNet represents a lightweight yet highly effective framework, setting a new benchmark in modern spatial-domain steganalysis research.

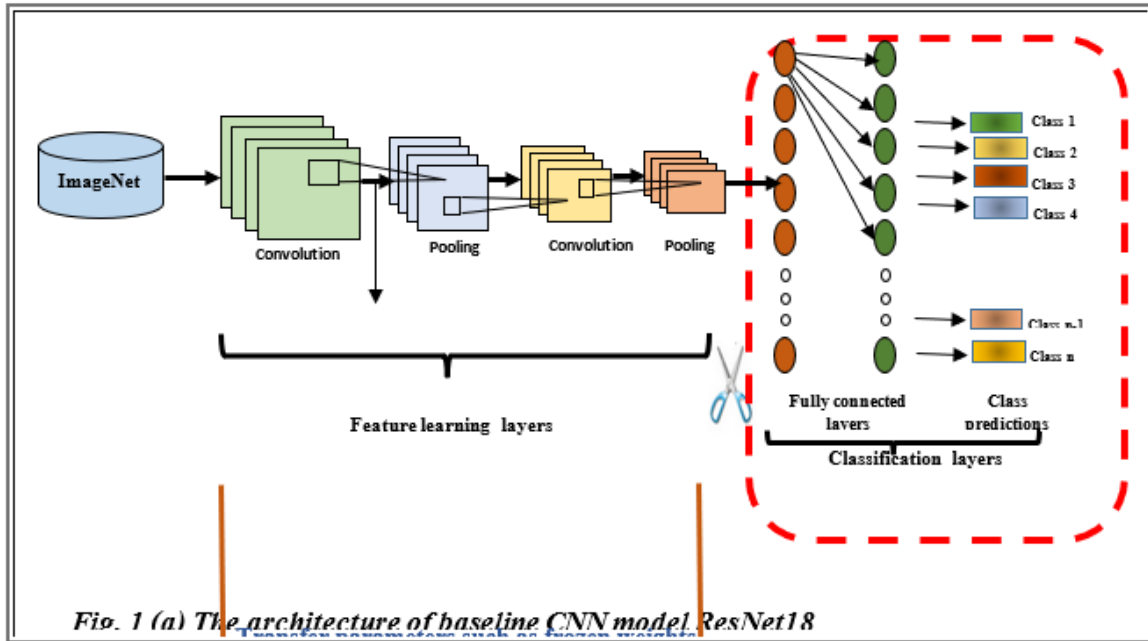


Fig. 1 (a) The architecture of baseline CNN model ResNet18

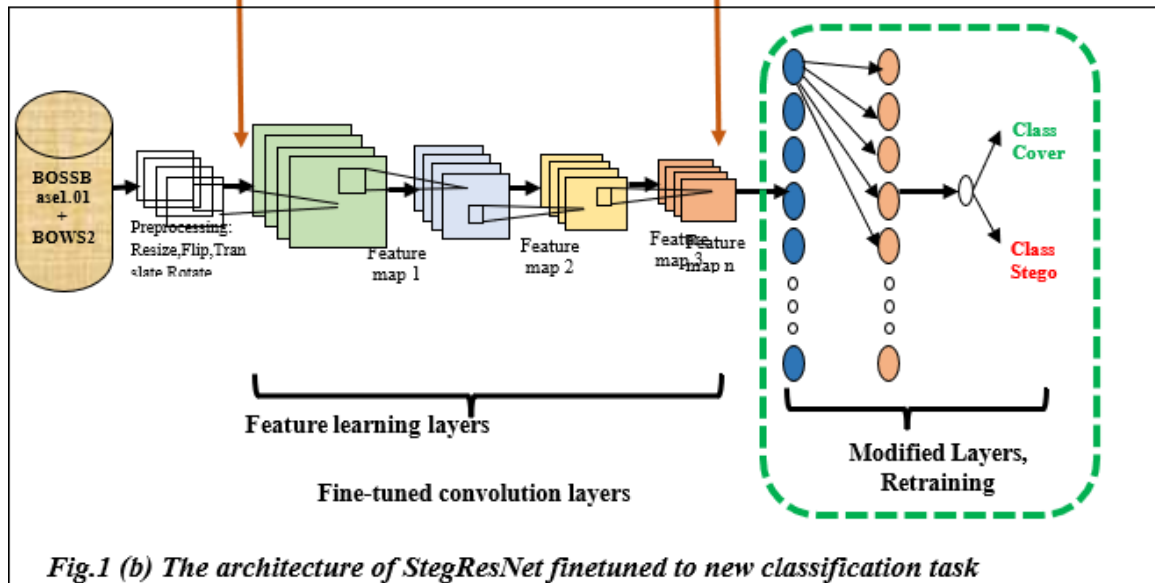


Fig.1 (b) The architecture of StegResNet finetuned to new classification task

Fig.1(a) The architecture of baseline CNN model ResNet18 **(b)** Tailored ResNet18 architecture named as StegResNet. The classification layer as shown in (a) is removed and the frozen weights are transferred to the new model and then fine-tuned for classification of images as Stego and Cover

3.1 Algorithmic Workflow of the Proposed StegResNet Framework

The proposed StegResNet model employs a structured workflow combining residual learning, transfer learning, and fine-tuned optimization to enhance spatial-domain image steganalysis. The following pseudocode (Algorithm) outlines the complete pipeline, followed by a detailed explanation of each stage.

Algorithm : Training and Validation Process of StegResNet	
Input:	
$D = \{C, S\}$	- Cover and Stego image datasets (BOSSBase1.01 + BOWS2)
$W_{pretrained}$	- Pretrained ResNet18 weights (ImageNet)
$H = \{\eta, B, E, M\}$	- Hyperparameters: Learning rate $\eta = 0.001$, Batch size $B = 32$, Epochs $E = 15$, Momentum $M = 0.9$
Output:	
M^*	- Optimized StegResNet model
Step 1: Data Preprocessing	
For each image $I \in D$ do	
Convert I to grayscale	
Resize I to 224×224 pixels	

Apply data augmentation (random rotation, horizontal flip) End For Split D into Training (70%), Validation (15%), and Test (15%) sets
Step 2. Model Initialization Load ResNet18 architecture pretrained on ImageNet Freeze initial convolutional layers to preserve generic low-level features Replace final fully connected layer with: Dropout ($\rho = 0.5$) Fully connected layer (2 output neurons) Softmax activation Define loss function $L = CrossEntropyLoss()$ Initialize optimizer = $SGD(\eta = 0.001, momentum = 0.9)$
Step 3 : Training Phase For $epoch = 1$ to E do For each mini-batch $x_{batch}, y_{batch} \in Training\ set$ do Forward Pass: $y_{pred} \leftarrow M(x_{batch})$ Compute loss: $\ell \leftarrow L(y_{pred}, y_{batch})$ Backward Pass: Compute gradients $\nabla \ell$ Update model parameters via SGD End For Evaluate model on Validation set Record metrics: Accuracy, Precision, Recall, F1-score End For
Step 4: Model Evaluation Evaluate optimized model M^* on Test set Compute final metrics: $Accuracy = \frac{(TP + TN)}{(TP + TN + FP + FN)}$ $Precision = \frac{TP}{(TP + FP)}$ $Recall = \frac{TP}{(TP + FN)}$ $F1 - Score = \frac{2 \times (Precision \times Recall)}{(Precision + Recall)}$ Report overall detection accuracy and confusion matrix Return M^*

The pseudocode above formally encapsulates the training and optimization pipeline of the proposed StegResNet model for spatial-domain image steganalysis. The process integrates residual learning, transfer-based fine-tuning, and efficient optimization to enhance feature discriminability and detection accuracy while maintaining computational efficiency. The complete workflow is divided into four primary stages.

3.1.1 Data Preprocessing and Augmentation

The input dataset $D = \{C, S\}$ comprises cover (C) and stego (S) images sourced from the BOSSBase v1.01 and BOWS2 datasets. These images represent benchmark samples widely used in spatial domain steganalysis research. Each image is converted to grayscale and resized from 512×512 to 224×224 pixels, conforming to the input requirements of the pretrained ResNet18 architecture. To enhance model robustness and mitigate overfitting, data augmentation techniques such as random rotation and horizontal flipping are applied. This step introduces geometric diversity and improves generalization by simulating varied embedding distortions. The dataset is then partitioned into training (70%), validation (15%), and test (15%) subsets, ensuring unbiased evaluation of the model's learning capability.

3.1.2 Model Initialization and Architectural Adaptation

The StegResNet framework builds upon the ResNet18 architecture pretrained on the ImageNet dataset. These pretrained weights $W_{pretrained}$ provide a strong initialization, allowing the model to leverage hierarchical spatial features and accelerate convergence. The initial convolutional layers of the pretrained ResNet18 are frozen to retain low-level spatial features—edges, contours, and textural gradients—that remain invariant across domains. The final fully connected (FC) layer is restructured to perform binary classification between cover and stego images. The newly added classification head includes:

- A Dropout layer with $\rho = 0.5$ to prevent co-adaptation and overfitting,
- A Fully Connected layer with two output neurons, and

- A Softmax activation function to produce normalized class probabilities.

The CrossEntropyLoss function is used as the objective criterion for classification, while Stochastic Gradient Descent (SGD) with learning rate ($\eta = 0.001$) and momentum ($M = 0.9$) serves as the optimizer. The model's total parameter count (≈ 11.18 million) provides a balanced trade-off between representational power and computational cost.

3.1.3 Training and Optimization Phase

The training process proceeds iteratively for $E = 15$ epochs, with a batch size (B) = 32. In each iteration, mini-batches of training data are passed through the network in two main computational steps:

Forward Pass:

The input mini-batch x_{batch} is propagated through the network to obtain predicted outputs y_{pred} . The cross-entropy loss is then computed by eq. 2:

$$\ell \leftarrow L(y_{pred}, y_{batch}) \quad (2)$$

which quantifies the divergence between predicted and actual labels.

Backward Pass

The gradient of the loss function $\nabla \ell$ with respect to model parameters is computed via backpropagation, and the parameters are updated using the SGD optimization rule as expressed by eq. 3:

$$w_{t+1} = w_t - \eta (\nabla \ell_t + M \cdot \Delta w_{t-1}) \quad (3)$$

This update mechanism ensures efficient gradient propagation and mitigates oscillations during convergence. After each epoch, the model's performance is validated on the validation subset, and key evaluation metrics accuracy, precision, recall, and F1-score are recorded to monitor the learning dynamics and prevent overfitting.

3.1.4 Model Evaluation and Performance Assessment

Upon convergence, the optimized model M^* is evaluated using the test dataset. The quantitative performance is assessed using standard classification metrics defined by eq (4), (5), (6) and (7):

$$Accuracy = \frac{(TP + TN)}{(TP + TN + FP + FN)} \quad (4)$$

$$Precision = \frac{TP}{(TP + FP)} \quad (5)$$

$$Recall = \frac{TP}{(TP + FN)} \quad (6)$$

$$F1 - Score = \frac{2 \times (Precision \times Recall)}{(Precision + Recall)} \quad (7)$$

where TP, TN, FP and FN denote true positive, true negative, false positive, and false negative counts, respectively.

The proposed StegResNet achieves a detection accuracy of 91.27% on the combined BOSSBase and BOWS2 datasets, surpassing established deep CNN steganalyzers such as YeNet, YedroudjNet, SRNet, ZhuNet, and GBASNet. Its superior performance stems from the synergistic fusion of residual and transfer learning, which facilitates efficient gradient propagation, preserves high-frequency stego perturbations, and enhances generalization across varied embedding algorithms and payload capacities. The accompanying pseudocode and implementation framework underscore the technical robustness of StegResNet, reflecting its capability to integrate residual feature preservation, transfer-based initialization, and optimized fine-tuning within a compact architecture. Overall, the model demonstrates an effective balance between accuracy, computational efficiency, and scalability, establishing a robust and extensible foundation for future research in spatial-domain steganalysis and digital forensics.

4. Experimental Results and Discussion

4.1 Software and Hardware

The proposed CNN architecture was developed using Python 3.10 and designed with PyTorch. The implementation was executed on a workstation running Ubuntu 22.04 with an AMD Threadripper Pro. The implementation utilized the Google Colaboratory platform in an environment equipped with an RTX 4090 GPU, CUDA 12.3, and 128 GB of RAM.

4.2 Dataset and partition

4.2.1 Benchmark datasets

Our experiments utilizes two benchmark datasets widely used to evaluate the performance of steganographic algorithms and steganalysis methods, BOSSBase1.01 and BOWS2 each of which contains 10,000 cover images in PNG format, each with a resolution of 512 x 512 pixels and bits in grayscale.

4.2.2 Dataset partition

The dataset, consisting of both cover and stego images, is partitioned into three subsets to ensure robust model training and evaluation. The training set (70%) is used to learn discriminative features by optimizing network parameters, while the validation set (20%) facilitates hyperparameter tuning and performance monitoring during training. The test set (10%,) is reserved for evaluating the generalization capability of the finalized model on unseen data.

4.3 Steganography algorithms

Five spatial domain content adaptive [35-36] steganographic algorithms were used to embed noise in the cover images from the databases; these were: WOW, S-UNIWARD, HUGO, MiPOD and HILL with two payloads 0.2 and 0.4 bpp.

4.4 Performance metrics

4.4.1 Confusion Matrix Analysis

To evaluate the classification capability of the proposed StegResNet model, a confusion matrix was computed on the test dataset to analyze the class-wise predictions for *cover* and *stego* images. This matrix provides a detailed view of correctly and incorrectly classified samples, thereby enabling an in-depth understanding of the model's discriminative ability. The class-wise statistics are summarized as follows:

- **True Positives (TP):** 5881 for *cover* and 6951 for *stego* images, instances where predictions match the actual labels.
 - **False Positives (FP):** 43 for *cover* and 1125 for *stego*, cases of incorrect classification across the two classes.
 - **False Negatives (FN):** 1125 for *cover* and 43 for *stego*, misclassified instances in the opposite direction.
 - **True Negatives (TN):** 6951 for *cover* and 5881 for *stego*, correctly rejected samples of the opposite class.
- Based on Table 2, the quantitative evaluation of the model in terms of accuracy, precision, recall, and F1-score is summarized in Table 3. The proposed StegResNet achieves an overall accuracy of 91.65%, reflecting its strong classification ability. For the *cover* class, a precision of 99.27% and recall of 83.94% indicate excellent reliability with minimal false detections. The *stego* class exhibits a precision of 86.06% and an outstanding recall of 99.38%, confirming that nearly all stego instances are successfully detected. The corresponding F1-scores 90.96% for *cover* and 92.24% for *stego* demonstrate balanced precision–recall trade-offs and robust generalization across both classes.

		Predicted Labels	
		Cover	Stego
Actual Labels	Cover	5881	1125
	Stego	43	6951

Table 2. Confusion Matrix for StegResNet evaluated on the steganographic algorithms WOW, S-UNIWARD, HUGO, MiPOD, and HILL with payloads of 0.2bpp and 0.4bpp, utilizing the BOSSbase v1.01 and BOWS2 datasets

Performance metrics	StegResNet	
	Class Cover	Class Stego
Accuracy (overall)	91.65%	
Precision	99.27%	86.06%
Recall	83.94%	99.38%
F1 Score	90.96%	92.24%

Table 2 Percentage values for various performance metrics, showcasing the model's effectiveness in terms of accuracy, precision, recall, and F1 score

4.5 Comparison with State-of-the-art approaches

To demonstrate the superiority of the proposed StegResNet, its performance was compared with several established CNN-based steganalyzers. Table 3 presents the comparative detection accuracies across prominent architectures such as SRNet, YedroudjNet, GBRASNet, and ZhuNet. StegResNet achieved a detection accuracy of 91.27%, significantly outperforming existing architectures GBRASNet (77.9%), ZhuNet (75.7%), SRNet (70.1%), YedroudjNet (65.9%), and YeNet (65.1%).

This improvement can be attributed to the incorporation of transfer learning, optimized residual feature extraction, and fine-tuning of deeper convolutional layers, which collectively enhance feature discrimination between cover and stego samples. The superior performance demonstrates that StegResNet efficiently captures subtle pixel-domain discrepancies introduced by different embedding algorithms and payload intensities.

Architecture	Detection Accuracy
StegResNet (2024)	91.27 %
GBRASNet (2020) [12]	77.9 %
ZhuNet (2019) [11]	75.7 %
SRNet(2018) [10]	70.1 %
YedroudjNet (2018) [9]	65.9 %
YeNet (2017) [8]	65.1 %

Table 3 Comparative performance of StegResNet with existing state-of-the-art CNN-based steganalyzers using combined BOSSBase 1.01 and BOWS2 datasets. Bold accuracy denotes superior performance of the proposed model.

4.6 Training Dynamics and Convergence Behavior

The StegResNet model was trained over 15 epochs with a learning rate of 0.001 and SGD optimizer (momentum = 0.9). The dataset was split into training, validation, and test subsets. Each experiment was repeated 15 times to ensure consistency. The training and validation performance across epochs is detailed in Table 7.

During experiments, the dataset was split into training, testing, and validation sets, and the model training was repeated 15 times to obtain the showcased result. The outcomes of our model using transfer learning are displayed in Table 7. The proposed model StegResNet achieved an overall accuracy of 91.27%, with the test set accuracy at 91.27%. The total training time for the model was 20 minutes and 40 seconds. The highest validation accuracy achieved was 91.2656%, as shown in the Table 7. Also the performance of our proposed model in each epoch was tracked down. It was observed that, the loss decreased with the epoch and then stabilized in train set and validation set as shown in Fig. 3(a). The accuracy increased with the epoch and then stabilized in train set and validation set as illustrated in Fig. 3(b). The graphs depicted in Fig. 3 (a) and (b) provides a visual representation of how the model's loss changes and converges over epochs for both training and validation sets. Fig. 3(a) Training and Validation Loss over Epochs for CNN Model: This graph illustrates the loss values for the training and validation datasets as the number of epoch increases. The blue line indicates training loss, and the orange line represents validation loss.

Epoch	Training Loss / Accuracy	Validation Loss / Accuracy
0 / 14	0.4103 / 0.8078	0.4655 / 0.7826
1 / 14	0.3162 / 0.8688	0.3646 / 0.8443
2 / 14	0.2923 / 0.8826	0.3414 / 0.8556
3 / 14	0.2776 / 0.8911	0.5719 / 0.7049
4 / 14	0.2690 / 0.8958	0.3180 / 0.8661
5 / 14	0.2616 / 0.9000	0.2885 / 0.8855
6 / 14	0.2560 / 0.9028	0.3869 / 0.8280
7 / 14	0.2434 / 0.9097	0.2474 / 0.9076
8 / 14	0.2384 / 0.9126	0.2474 / 0.9084
9 / 14	0.2368 / 0.9133	0.2431 / 0.9115
10 / 14	0.2354 / 0.9138	0.2413 / 0.9116
11 / 14	0.2356 / 0.9136	0.2411 / 0.9117
12 / 14	0.2351 / 0.9140	0.2402 / 0.9109
13 / 14	0.2351 / 0.9139	0.2543 / 0.9034
14 / 14	0.2325 / 0.9157	0.2390 / 0.9127

Table 7 Epoch-wise training and validation performance of StegResNet

A steadily decreasing loss, as shown in Fig. 3(a), demonstrates that the model is effectively learning and optimizing. As epochs progress, the loss values plateau, indicating that the model has reached its optimal learning capacity given the data and architecture. The close alignment and tandem decrease of training and validation loss demonstrates good generalization. Fig. 3(b) Training and Validation Accuracy over Epochs for CNN Model: This graph displays the accuracy values for both the training and validation datasets across different epochs. The blue line indicates the training accuracy, and the orange line represents the validation accuracy. An increasing training accuracy over epochs indicates that the model is learning patterns in the training data. The rising validation accuracy suggests that the model is generalizing well to unseen data. The point where the training and validation accuracy curves level off indicates model convergence. Further training beyond this point did not yield significant improvements in accuracy and hence further training was stopped. As evident from Fig. 3(b), a steady increase in both training and validation accuracy, eventually plateauing over epochs, indicates that the model is learning effectively and generalizing properly.

The loss and accuracy trends across epochs are illustrated in Fig. 3(a) and Fig. 3(b), respectively. The training and validation losses exhibit a consistent downward trend, eventually stabilizing after the 10th epoch,

indicating that the network effectively converges without overfitting. Simultaneously, the accuracy curves demonstrate a steady increase followed by saturation, implying optimal learning and generalization.

The close correspondence between training and validation metrics confirms that the model maintains strong bias–variance balance, learning discriminative representations without memorizing noise. The final test accuracy of 91.27% validates the network’s ability to generalize to unseen stego artifacts, confirming the robustness of the architecture for Spatial domain steganalysis.\

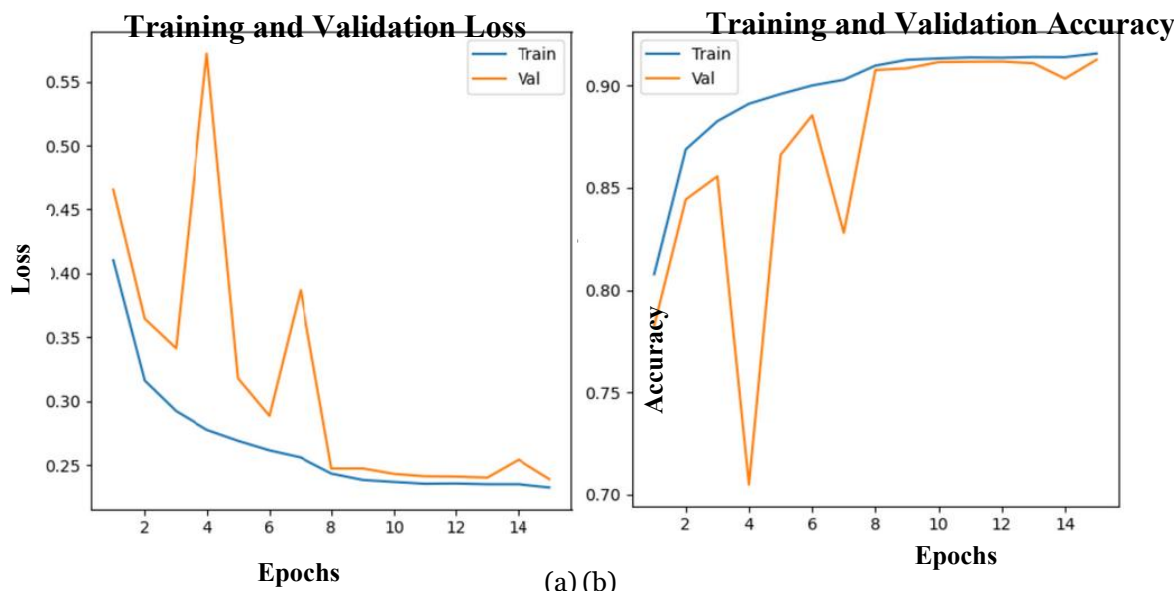


Fig.3(a) Training dynamics of StegResNet: (a) Loss vs. Epochs; (b) Accuracy vs. Epochs for training and validation on BOSSBase 1.01 + BOWS2 datasets.

In summary, the proposed StegResNet demonstrates:

- Stable and convergent learning behavior across epochs,
- Superior classification accuracy (91.27%) compared to existing CNN-based methods, and
- Robust generalization on complex, payload-variable stego datasets.

These results collectively validate the model’s capability to serve as an effective, lightweight, and high-performing architecture for Spatial domain image steganalysis.

4.7 Result and discussions

The proposed StegResNet achieves superior steganalytic performance through an optimized integration of residual learning and transfer learning, enabling robust feature generalization across multiple embedding algorithms and payloads. By leveraging ImageNet-pretrained ResNet18 weights, the model effectively reuses low-level spatial features (edges, textures, and gradients), accelerating convergence and enhancing sensitivity to subtle embedding distortions. Its residual blocks ensure stable gradient flow, mitigate vanishing gradient issues, and preserve high-frequency stego artefacts critical for accurate detection.

Fine-tuned layer freezing and selective retraining achieve an optimal trade-off between model depth and computational efficiency, enhancing discriminative power while minimizing overfitting. Multi-scale feature fusion further strengthens class separability between cover and stego representations. Empirical results demonstrate consistent detection accuracy across diverse steganographic algorithms WOW, S-UNIWARD, HUGO, MiPOD, and HILL and payload rates (0.2, 0.4 bpp), achieving 91.27% accuracy with a low detection error rate.

The lightweight architecture, high precision–recall balance, and transferable feature hierarchy position StegResNet as a scalable, interpretable, and computationally efficient framework for spatial-domain steganalysis, establishing a strong foundation for future advancements in forensic and cybersecurity applications.

5. Conclusion and Future directions

A novel framework “StegResNet” employing embodiment of residual learning and transfer of pre-trained validated reference model’s knowledge is proposed. The notion behind this strategy is that integrating knowledge transfer and skip connections of pretrained model ResNet18 can improve performance. The model’s lightweight architecture, coupled with careful hyperparameter tuning and fine-tuning, enhances its capacity to capture intricate features and patterns, yielding superior performance in comparison to SOTA CNN based steganalyzer models. The proposed architecture StegResNet is developed for detection of steganographic

images with improved accuracy in comparison to the notable architectures YeNet, YedroudjNet, SRNet, ZhuNet and GBRASNet reported in the literature. The strategy proposed for binary image classification using CNN were trained and tested on benchmark dataset (both cover and stego images) BOSSBase 1.01 + BOWS2 with spatial steganographic algorithms WOW, S-UNIWARD, HUGO, MiPOD and HILL with payloads of 0.2bpp and 0.4bpp, respectively and also on unseen samples. The popular evaluation metrics used as fitness criteria were accuracy of 91.65%, precision rates of 99.27% for the cover class and 86.06% for the stego class, and recall rates of 83.94% for the cover class and 99.38% for the stego class respectively. The results revealed that the our model surpasses the performance on the classification as against existing SOTA CNN based models in terms of accuracy as demonstrated in Table 7. This research represents a significant step towards achieving superior results in stego-cover image classification and paves the way for future advancements in lightweight architectures.

In future work, the model can be extended to cross-domain and adaptive steganalysis scenarios by incorporating attention mechanisms and multi-scale feature fusion to enhance generalization to unseen steganographic algorithms. Additionally, integrating transformer-based architectures and exploring frequency-domain feature fusion may further boost discriminative capability. The proposed framework thus lays a robust foundation for next-generation universal steganalyzers capable of efficient and accurate detection of hidden information in diverse image domains.

Acknowledgements

Special thanks to Professor and Head of Department Information Technology Dr. Ani Thomas for data analysis and technical assistance. Her extraordinary contributions have greatly improved the quality of this research paper.

Statements and Declarations

Declaration of competing interest

The authors state that they have no conflicts of interest related to the publication of this paper.

Data availability

The datasets created and analysed during this development of model are available from the corresponding author upon reasonable request.

Funding

This research received no specific grant from any funding agency in the public, commercial, or not-for-profit sectors.

References

- [1] Ntivuguruzwa, J. D. L. C., Ahmad, T., & Han, F. (2024). Comprehensive survey on image steganalysis using deep learning. *Array*, 22, 100353. <https://doi.org/10.1016/j.array.2024.100353​>
- [2] K. He, X. Zhang, S. Ren, and J. Sun, "Deep residual learning for image recognition," in Proc. IEEE Conf. Comput. Vis. Pattern Recognit., 2016, pp. 770–778.
- [3] Qian, Y., Dong, J., Wang, W., & Tan, T. (2015, March). Deep learning for steganalysis via convolutional neural networks. In Proceedings of SPIE 9409, Media Watermarking, Security, and Forensics 2015 (Vol. 9409). <https://doi.org/10.1117/12.2083479>
- [4] Ozcan, S., & Mustacoglu, A. F. (2018, December). Transfer learning effects on image steganalysis with pre-trained deep residual neural network model. In 2018 IEEE International Conference on Big Data (Big Data) (pp. 2280-2287). IEEE.
- [5] H. Yang, H. He, W. Zhang and X. Cao, "FedSteg: A Federated Transfer Learning Framework for Secure Image Steganalysis," in IEEE Transactions on Network Science and Engineering, vol. 8, no. 2, pp. 1084-1094, 1 April-June 2021, doi: 10.1109/TNSE.2020.2996612.
- [6] Kadhim, I. J., Premaratne, P., Vial, P. J., Al-Qersh, O. M., & Al-Shebani, Q. (2020). Towards a Universal Steganalyser Using Convolutional Neural Networks. In Intelligent Computing Methodologies: 16th International Conference, ICIC 2020, Bari, Italy, October 2–5, 2020, Proceedings, Part III 16 (pp. 611-623). Springer International Publishing.
- [7] Fridrich, J., Kodovský, J., Holub, V., & Goljan, M. (2011). Steganalysis of content-adaptive steganography in spatial domain. In *Lecture Notes in Computer Science* (pp. 102–117). Springer Berlin Heidelberg.
- [8] J. Ye, J. Ni and Y. Yi, "Deep Learning Hierarchical Representations for Image Steganalysis," in *IEEE Transactions on Information Forensics and Security*, vol. 12, no. 11, pp. 2545-2557, Nov. 2017, doi: 10.1109/TIFS.2017.2710946.
- [9] M. Yedroudj, F. Comby and M. Chaumont, "Yedroudj-Net: An Efficient CNN for Spatial Steganalysis," 2018 IEEE International Conference on Acoustics, Speech and Signal Processing (ICASSP), Calgary, AB, Canada, 2018, pp. 2092-2096, doi: 10.1109/ICASSP.2018.8461438.

- [10] M. Boroumand, M. Chen and J. Fridrich, "Deep Residual Network for Steganalysis of Digital Images," in *IEEE Transactions on Information Forensics and Security*, vol. 14, no. 5, pp. 1181-1193, May 2019, doi: 10.1109/TIFS.2018.2871749
- [11] R. Zhang, F. Zhu, J. Liu and G. Liu, "Depth-Wise Separable Convolutions and Multi-Level Pooling for an Efficient Spatial CNN-Based Steganalysis," in *IEEE Transactions on Information Forensics and Security*, vol. 15, pp. 1138-1150, 2020, doi: 10.1109/TIFS.2019.2936913.
- [12] Reinel, T.-S., Tabros, R., & others. (2021). GBRAS-Net: A convolutional neural network architecture for spatial image steganalysis. *IEEE Access*, 9, 14340-14350. <https://doi.org/10.1109/ACCESS.2021.3052494>
- [13] C. V. Priscilla and V. HemaMalini, "Effective Analysis of Real World Stego Images through Deep Learning Techniques," 2024 3rd International Conference on Applied Artificial Intelligence and Computing (ICAAIC), Salem, India, 2024, pp. 780-785, doi: 10.1109/ICAAIC60222.2024.10575850.
- [14] Avcibas, I., Memon, N., & Sankur, B. (2003). Steganalysis using image quality metrics. *IEEE transactions on image processing : a publication of the IEEE Signal Processing Society*, 12 2, 221-9 .
- [15] Goljan, M., Fridrich, J., & Holotyak, T. (2006). New blind steganalysis and its implications. *Electronic Imaging*.
- [16] Tabares Soto, Reinel & Pollán, Raúl & Isaza, Gustavo. (2019). Deep Learning Applied to Steganalysis of Digital Images: A Systematic Review. *IEEE Access*. PP. 1-1. 10.1109/ACCESS.2019.2918086.
- [17] Agarwal, Saurabh, Cheonshik Kim, and Ki-Hyun Jung. 2022, Steganalysis of Context-Aware Image Steganography Techniques Using Convolutional Neural Network", *Applied Sciences* 12, no. 21: 10793, <https://doi.org/10.3390/app122110793>.
- [18] Su, H., Han, M., Liang, J., & Yu, S. (2022). Steganalysis of Image with Adaptively Parametric Activation. *ArXiv*, abs/2203.12843
- [19] R. Zhang, F. Zhu, J. Liu, and G. Liu, "Depth-wise separable convolutions and multi-level pooling for an efficient spatial CNN-based steganalysis," *IEEE Transactions on Information Forensics and Security*, vol. 15, pp. 1138-1150, 2020.
- [20] He, K., Zhang, X., Ren, S., & Sun, J. (2015). Spatial Pyramid Pooling in Deep Convolutional Networks for Visual Recognition. *IEEE Transactions on Pattern Analysis and Machine Intelligence*, 37, 1904-1916.
- [21] T. Denemark, V. Sedighi, V. Holub, R. Cogranne and J. Fridrich, "Selection-channel-aware rich model for Steganalysis of digital images," 2014 IEEE International Workshop on Information Forensics and Security (WIFS), Atlanta, GA, USA, 2014, pp. 48-53, doi: 10.1109/WIFS.2014.7084302.
- [22] G. Xu, H.-Z. Wu, and Y.-Q. Shi, "Structural design of convolutional neural networks for steganalysis," *IEEE Signal Process. Lett.*, vol. 23, no. 5, pp. 708-712, May 2016.
- [23] J. Zeng, S. Tan, B. Li, and J. Huang, "Large-scale JPEG image steganalysis using hybrid deep-learning framework," *IEEE Transactions on Information Forensics and Security*, vol. 13, pp. 1200-1214, May 2018.
- [24] Luo, G., Wei, P., Zhu, S., Zhang, X., Qian, Z., & Li, S. (2022, May). Image steganalysis with convolutional vision transformer. In *ICASSP 2022-2022 IEEE International Conference on Acoustics, Speech and Signal Processing (ICASSP)* (pp. 3089-3093). IEEE.
- [25] F. Liu, X. Zhou, X. Yan, Y. Lu, and S. Wang, "Image Steganalysis via Diverse Filters and Squeeze-and-Excitation Convolutional Neural Network," 2021.
- [26] Mikołajczyk and M. Grochowski, "Data augmentation for improving deep learning in image classification problem," 2018 International Interdisciplinary PhD Workshop (IIPHDW), Świnouście, Poland, 2018, pp. 117-122, doi: 10.1109/IIPHDW.2018.8388338.
- [27] Yedroudj, M., Chaumont, M., Comby, F., Amara, A.O., & Bas, P. (2020). Pixels-off: Data-augmentation Complementary Solution for Deep-learning Steganalysis. *Proceedings of the 2020 ACM Workshop on Information Hiding and Multimedia Security*.
- [28] Itzhaki, T., Yousfi, Y., & Fridrich, J. (2021, December). Data augmentation for JPEG steganalysis. In *2021 IEEE International Workshop on Information Forensics and Security (WIFS)* (pp. 1-6). IEEE.
- [29] J. Deng, W. Dong, R. Socher, L.-J. Li, K. Li, and L. Fei-Fei, "ImageNet: A large-scale hierarchical image database," in *IEEE conference on computer vision and pattern recognition*, pp. 248-255, June 20-25, 2009.
- [30] Holub, V., & Fridrich, J. (2012, December). Designing steganographic distortion using directional filters. In *2012 IEEE International workshop on information forensics and security (WIFS)* (pp. 234-239). IEEE.
- [31] Holub, Vojtech & Fridrich, Jessica & Denemark, Tomáš. (2014). Universal Distortion Function for Steganography in an Arbitrary Domain. *EURASIP Journal on Information Security*. 1. 10.1186/1687-417X-2014-1.
- [32] T. Pevný, T. Filler, and P. Bas, "Using high-dimensional image models to perform highly undetectable steganography," in *Proc. Int. Workshop Inf. Hiding*, 2010, pp. 161-177.
- [33] V. Sedighi, R. Cogranne, and J. Fridrich, "Content-adaptive steganography by minimizing statistical detectability," *IEEE Trans. Inf. Forensics Security*, vol. 11, no. 2, pp. 221-234, Feb. 2016.
- [34] Li, B., Wang, M., Huang, J., & Li, X. (2014). A new cost function for spatial image steganography. *2014 IEEE International Conference on Image Processing (ICIP)*, 4206-4210.

- [35] Swarnkar, Neelam & Thomas, Ani & Selwal, Arvind. (2023). A generalized image steganalysis approach via decision level fusion of deep models. *Multimedia Tools and Applications*. 83. 10.1007/s11042-023-17068-0.
- [36] Swarnkar, N., Rawal, A., & Patel, G. (2021). A paradigm shift for computational excellence from traditional machine learning to modern deep learning-based image steganalysis. In *Data science and innovations for intelligent systems* (1st ed., pp. 32). CRC Press. <https://doi.org/10.1201/9781003132080>
- [37] Qian, Yinlong & Dong, Jing & Wang, Wei & Tan, Tieniu. (2016). Learning and transferring representations for image steganalysis using convolutional neural network. 2752-2756. 10.1109/ICIP.2016.7532860.
- [38] Agarwal, Saurabh & Kim, Cheonshik & Jung, Ki-Hyun. (2022). Steganalysis of Context-Aware Image Steganography Techniques Using Convolutional Neural Network. *Applied Sciences*. 12. 10793. 10.3390/app122110793.
- [39] Agarwal, Saurabh & Jung, Ki-Hyun. (2022). Identification of Content-Adaptive Image Steganography Using Convolutional Neural Network Guided by High-Pass Kernel. *Applied Sciences*. 12. 11869. 10.3390/app122211869.
- [40] Luo, G., Wei, P., Zhu, S., Zhang, X., Qian, Z., & Li, S. (2022, May 23–27). Image steganalysis with convolutional vision transformer. In *Proceedings of the 2022 IEEE International Conference on Acoustics, Speech and Signal Processing (ICASSP)* (pp. 3089–3093). IEEE. <https://doi.org/10.1109/ICASSP43922.2022.9747091>
- [41] Deng, X.-Q., Chen, B.-L., Luo, W.-Q., & Luo, D. (2022). Universal image steganalysis based on convolutional neural network with global covariance pooling. *Journal of Computer Science and Technology*, 37(5), 1134–1145. <https://doi.org/10.1007/s11390-021-0572-0>